HHS Public Access

Author manuscript

J Immunol. Author manuscript; available in PMC 2016 April 01.

Published in final edited form as:

J Immunol. 2015 April 1; 194(7): 3035–3044. doi:10.4049/jimmunol.1402690.

TLR7 and TLR9 responsive human B cells share phenotypic and genetic characteristics

Noa Simchoni and **Charlotte Cunningham-Rundles**

Division of Clinical Immunology, Department of Medicine, Icahn School of Medicine at Mount Sinai, New York, NY, USA

Abstract

B cells activated by nucleic-acid sensing Toll-like receptor 7 and TLR9 proliferate and secrete immune globulins. Memory B cells are presumably more responsive due to higher TLR expression levels, but selectivity and differential outcomes remain largely unknown. In this study, peripheral blood human B cells were stimulated by TLR7 or TLR9 ligands, with or without IFNα, and compared to activators CD40L plus IL-21, to identify differentially responsive cell populations, defined phenotypically and by BCR characteristics. While all activators induced differentiation and antibody secretion, TLR stimulation expanded IgM+ memory and plasma cell lineage committed populations and favored secretion of IgM, unlike CD40L/IL-21 which drove IgM and IgG more evenly. Patterns of proliferation similarly differed, with CD40L/IL-21 inducing proliferation of most memory and naïve B cells, in contrast to TLRs which induced robust proliferation in a subset of these cells. On deep sequencing of the IgH locus, TLR responsive B cells shared patterns of IgHV and IgHJ usage, clustering apart from CD40L/IL-21 and control conditions. TLR activators, but not CD40L/IL-21, similarly promoted increased sharing of CDR3 sequences. TLR responsive B cells were characterized by more somatic hypermutation, shorter CDR3 segments, and less negative charges. TLR activation also induced long positively charged CDR3 segments, suggestive of autoreactive antibodies. Testing this, culture supernatants from TLR stimulated B cells were found to bind HEp-2 cells, while those from CD40L/IL-21 stimulated cells did not. Human B cells possess selective sensitivity to TLR stimulation, with distinctive phenotypic and genetic signatures.

Keywords

Animals-Human; Cells-B Cells; Molecules-Autoantibodies; Processes-Memory; Processes-Cell Activation; Toll Like Receptors; High Throughput Sequencing

Corresponding Author: Charlotte Cunningham-Rundles, MD, PhD, Division of Clinical Immunology, Department of Medicine, Icahn School of Medicine at Mount Sinai, 1425 Madison Ave, New York, NY 10029, Telephone: 212-659-9243, Fax: 212-987-5593, charlotte.cunningham-rundles@mssm.edu.

PC: plasma cell
SHM: somatic hypermutation
NA: natural antibody

Introduction

B cells are commonly activated by antigen and co-stimulated by CD40-ligand and cytokines in germinal centers; however, B cells can also be activated by selected toll like receptors agonists, leading to enhanced cell survival, proliferation, secretion of IL-6 and IL-10, isotype switch, and differentiation into immune globulin producing plasma cells (1–3). Naïve human B cells express low levels of TLRs 1, 6, 7, 9, and 10, while CD27+ memory B cells have increased receptor expression, especially of TLRs 7 and 9 (4) activated by single-stranded RNA or by un-methylated CpG motifs from microbial DNA. For stimulation using TLR7 agonists, removal of plasmacytoid dendritic cells reduced Ig production, while the addition of IFN-α, a transcriptional upregulator of TLRs (1), restored Ig secretion, suggesting that IFN-α is important for TLR7 driven antibody production. IFN-α similarly boosted responses of naïve B cells to TLR9 agonists (5). TLR9 stimulation of human B cells induced IgM+ memory B cells to secrete anti-carbohydrate antibodies of the IgM isotype (6, 7) and other IgM antibodies of broad specificity (8). These human B cells responses thus resemble well-characterized responses of murine innate-like B populations, namely B1 and splenic marginal zone B cells, both of which respond to TLR stimulation with rapid and high-titer antibody secretion (9–11). While human peripheral blood IgM+ memory B cells are not directly analogous to non-circulating rodent B1 or marginal zone B cells (12, 13), TLR9 stimulation nevertheless induces this population to secrete anti-carbohydrate and polyspecific IgM, consistent with the reactivities of “natural” antibodies that may provide early protection against bacterial infections (11, 14).

While memory B cells, and especially IgM+ memory B cells, are activated by TLR triggers, how TLR-responsive B cells might differ from T cell activated B cells, in terms of BCR structure, immune globulin isotype production, and antibody specificity, has remained undefined. In this study, we have examined the hallmarks of TLR responsive human peripheral blood B cells from healthy donors, assessing the responding cell phenotypes, production of immune globulin isotypes, and BCR characteristics as determined by deep sequencing. As a contrast, we compared TLR responding cells to B cells responding to CD40L and IL-21 co-stimulation, a mimic of the germinal center environment. We found that TLR7 and 9 activation expanded IgM+ memory (CD27+) and plasma cell (PC) lineage committed ($CD27^{hi}$) populations (15), resulting in preferential IgM secretion, unlike CD40L/IL-21 stimulation which activated IgM- memory and PC committed populations and induced more equal IgM and IgG production. The BCRs of TLR responsive B cells also shared patterns of IgHV and IgHJ usage, were more likely to have undergone somatic hypermutation (SHM), and had shorter CDR3 segments with a less negative charge, unlike CD40L/IL-21 activated cells which lacked these characteristics. TLR-activated B cells also produced HEp-2 reactive autoantibodies not seen following CD40L/IL-21 stimulation. Thus, increased TLR responsiveness may define a subset of B cells with unique biological capacities.

Materials and Methods

Blood and B cell isolation

De-identified leukocyte concentrates were obtained from four healthy blood donors from the New York Blood Center. PBMCs were isolated from these by centrifugation over Ficoll-Paque (GE Healthcare, Uppsala, Sweden), and B cells isolated by negative magnetic selection using the human B Cell Isolation Kit II (Miltenyi Biotec, San Diego, CA).

Culture and stimulation conditions

Agonists included a TLR7 agonist imidazoquinoline compound (Clo97), used at 250ng/mL, and a TLR9 CpG-B agonist (ODN2006), used at 300ng/mL (InvivoGen, San Diego, CA). Additional TLR cultures included IFNα at 1000U/mL (Schering, Kenilworth, NJ) to maximize TLR responses (5). To mimic T follicular helper cell activation, B cells were cultured with 150ng/mL of trimerized recombinant human CD40L (Enzo Life Sciences, Farmingdale, NY) in conjunction with 10ng/mL of recombinant human IL-21 (Cell Signaling, Danvera, MA) (16). Culture media consisted of RPMI 1640 (Cellgro, Herndon, VA) supplemented with 10% inactivated fetal bovine serum (Atlanta Biologicals, Lawrenceville, GA), and 1% L-glutamine, HEPES, and antibacterial/antimycotic supplements (Life Technologies, Grand Island, NY). Cells were cultured in either U-bottom 96-well plates at a density of 1×10^5 in 200uL, or in 24-well plates at a density of 1.15×10^6 in 1mL (BD Biosciences, San Jose, CA). To assess proliferation, B cells were stained at baseline with Cell Trace CFSE (Life Technologies, Grand Island, NY) as per manufacturer instructions, and cultured for seven days in 96-well plates as above.

Flow cytometry

B cells were Fc blocked (BD Biosciences, San Jose, CA) prior to staining. Cells were analyzed using an LSR Fortessa cytometer (BD Biosciences), with gating performed by first setting a wide lymphocyte gate by forward and side scatter, followed by two sets of doublet exclusion, first by FSC-A by FSC-H and then by FSC-A by FSC-W, and by excluding dead cells with a viability stain (Life Technologies, Grand Island, NY). B cell purity was determined during isolation and at baseline by staining for CD19 (clone HIB19, eBiosciences, San Diego, CA). Cell phenotype was determined by staining IgM (clone MHM-88), CD27 (clone O323), and CD38 (clone HIT2, all from BioLegend, San Diego, CA), with results reported for the live cells gate. B cell proliferation was determined by dilution of CFSE dye, with results reported for the live singlet lymphocyte gate.

Immunoglobulin quantification

Total IgM and IgG levels in culture supernatants were quantified by ELISA (Bethyl Laboratories, Montgomery, TX), developed with TMB (BD Biosciences, San Jose, CA), stopped using 2N sulfuric acid (Sigma-Aldrich, St. Luis, MO), and read using the uQuant Microplate Reader (Bio-Tek, Winooski, VT).

HEp-2 staining

30uL of undiluted culture supernatants were tested for presence of autoreactive antibodies using HEp-2 slides and immunofluorescence reagents as per manufacturer instructions (MBL, Des Plaines, IL) for total Ig detection. A second slide was tested for IgM specific antibodies with FITC conjugated anti-human IgM (Dako, Denmark). Vectashield hardset mounting media (Vector Labs, Burlingame, CA) was used to prevent photobleaching while slides were read on an Axioplan 2 microscope (Zeiss, Jena, Germany). Interpretation of staining patterns was carried out based on descriptions provided by MBL in the product documentation.

IgH deep sequencing

Genomic DNA was isolated via centrifugation-based purification (ArchivePure, 5Prime, Hamburg), and 1μg (1 donor) or 2μg (3 donors) of DNA was frozen for survey-depth sequencing of the IgH locus (Adaptive Biotechnologies, Seattle, WA). Adaptive Biotechnologies performed the library generation, deep sequencing, and sequence filtering. The sequences obtained were processed with IMGT (17) to assign IgHV, IgHD, and IgHJ genes, delimit CDR3 boundaries, and annotate somatically hypermutated nucleotides. From 1μg of DNA from one donor, between 9,306 and 24,660 unique productive sequences were obtained (mean 17,335), while the other three donors had 17,500 to 70,500 unique productive sequences obtained from 2μg of DNA (mean 31,645). Total productive reads per sample ranged from 200,000 to 1,500,000 (mean = 679,334). Sequences that could not be assigned to IgHV and IgHJ families were not considered in the analyses, while those predicted to have stop codons or frame-shifts were used as false discovery internal controls.

Sequence analysis

Somatic hypermutation status was determined by mutations in the IgHV gene, with a mutated sequence being defined as containing 2 or more mutations to avoid potential mislabeling due to PCR artifacts. The IgHV gene was selected as it contains the most nucleotides and thus has the highest correct alignment probability in various alignment algorithms including IMGT (18). Analysis was performed using the programming language R (19), using the RStudio wrapper (20), and the plyr (21), stringr, ggplot2 (22), gplots, RColorBrewer, reshape (23), cluster (24), Interpol, and data.table packages. Unless otherwise indicated, analysis was performed on unique sequences to eliminate any bias arising from selective sequence amplification during sequencing. While PCR amplification might introduce such bias, the proprietary sequencing and filtering method used by Adaptive Biotechnologies corrects for PCR bias (25), thereby minimizing this concern. As such, differential impacts of stimulation on cell proliferation can be assessed by factoring in relative sequence frequencies as these are proportional to the number of input B cells bearing a given rearrangement in gDNA based sequencing.

Statistics

Statistical tests were performed in R or in Prism (Version 5, GraphPad, San Diego, CA). Results were first assessed by repeated-measure ANOVA, with Dunnett's multiple comparison tests as post hoc, using the unstimulated samples as controls. For differentiation

and immunoglobulin secretion, additional post hoc testing, with Dunnett's tests, was performed to compare results to CD40L/IL-21 treatment. With the exception of B differentiation and Ig secretion, following a significant ANOVA, samples were normalized to unstimulated samples by subtraction to directly assess the impact of stimulation while controlling for nonspecific effects of culture and for baseline differences between donors. Normalized results were tested with one-sample t tests versus the hypothetical mean of 0 to determine whether treatment led to any changes. Clustering was performed based on Euclidean distances and complete clustering using the heatmap.2 function from the gplots package. Given the potential for false discovery with any study of large datasets, identical analysis was performed on the unproductive sequence subset. Such sequences are bystanders, unshaped by selection and subject to expansion or contraction based on the independent productive rearrangement present in the same cell. Changes observed with TLR stimulation, such as gene usage and CDR3 charge and length characteristics, are not expected in these sequence repertoires. Changes relating to somatic hypermutation, meanwhile, are expected to appear as activation induced cytosine deaminase, the enzyme mediating SHM, induces mutations whenever the Ig locus is transcribed, which also occurs for nonproductive rearrangements. All findings reported follow these patterns, with results deviating from these patterns deemed to represent artifacts and excluded.

Results

TLR stimulation expands IgM+ memory, IgM+ plasma cell committed, and IgM secreting B cells

Peripheral blood B cells (>97% pure) of each donor were cultured with TLR7 and 9 agonists, with or without IFNα, or, for comparison, CD40/IL-21, to assess the relative frequencies of responding B cell populations. All stimulation conditions successfully induced B cell differentiation into $CD27^{hi}$ cells committed to the plasma cell (PC) lineage (Representative donor Figure 1A). The pattern of responses differed, however, with TLRs selectively expanding the proportion of IgM+ B cells among CD27+ memory populations (Figure 1B, ANOVA $p < 0.01$), represented as the change in proportion of IgM+ cells in the memory gate to control for baseline differences between donors. Similarly, TLRs selectively promoted IgM+ B cells and among $CD27^{hi}$ populations (Figure 1C, ANOVA $p < 0.0001$). CD40L/IL-21 stimulation, however, showed no selectivity among memory populations, and favored differentiation into class-switched IgM- $CD27^{hi}$ cells. Similarly, while all stimuli induced B cell proliferation, the patterns of proliferation were different (Representative donor Figure 2A). While CD40L/IL-21 induced proliferation of virtually all memory B cells and of a majority of naïve B cells, TLRs induced only a subset of these cells to divide. TLR responsive B cells, however, showed further dilution of CFSE, indicating more rounds of cell division. Despite the different proliferative responses, the proportion of live cells was largely similar among stimulated cells at the end of the culture (Figure 2B), as were the cell counts (data not shown).

Both TLRs and CD40L/IL-21 robustly induced secretion of IgM (Figure 3A, ANOVA $p < 0.0001$) and IgG was similarly secreted (Figure 3B, ANOVA $p < 0.0001$). Of note, TLRs

heavily skewed secretion towards IgM, while CD40L/IL-21 stimulation fostered relatively more balanced IgM and IgG production (Figure 3C, ANOVA p = 0.0037).

Deep Sequencing of the IgH locus reveals clustering of TLR stimulated cells based on V and J usage

To examine if TLR responsive B cells showed similar BCR structure, we performed deep sequencing of the Ig heavy chain locus of these cells to compare to those cultured with CD40L/IL-21. Figure 4A shows that, among mutated sequences, TLR9 and TLR/IFN stimulated cells from four donors shared similar changes in IgHV to IgHJ rearrangement frequencies, segregating these responders apart from CD40L/IL-21 stimulated and control cells. Similar clustering was obtained from repertoires that included nonmutated sequences, while clustering was weaker for repertoires of only nonmutated sequences (not shown). Analysis of BCR composition changes showed that TLR stimulation selectively expanded B cells bearing V3-J1, V3-J3, V3-J4, V3-J5, and V6-J4 rearrangements, at the expense of B cells bearing V1-J2, V1-J3, V1-J4, V1-J5, and V5-J4 rearrangements (Supplemental Table I). CD40L/IL-21 stimulation, on the other hand, expanded B cells bearing V1-J6 and V2-J6 rearrangements, but otherwise the repertoire did not differ from baseline B cells. Comparing sequences between donors also revealed that TLR stimulation, but not CD40L/IL-21, promoted expansion of B cells utilizing similar IgHV genes (Supplemental Table II).

This analysis highlights the impact of stimulation on cell survival as each rearrangement, regardless of its relative frequency, was given equal weight. When these analyses were corrected for relative sequence frequencies, thereby factoring in survival and proliferation, the changes in BCR composition promoted by TLR9 and TLR/IFN stimulation again clustered apart from sequences derived from both CD40L/IL-21 stimulated and control cells (not shown).

Changes in some IgHV genes have been reported to have associations with B cell subsets or functional outcomes. In particular, V1-69 was found in broadly neutralizing antibodies to influenza cloned from IgM+ memory B cells (26), and is overrepresented in nonmutated rearrangements in chronic lymphocytic leukemia (27). V3-30 has been found to be over-represented in B cells class switched to IgD (28), and has been associated with good prognosis in chronic lymphocytic leukemia (29). V4-34 has been shown to have autoimmune associations, particularly recognizing RBC antigens (30), while V4-39 was overrepresented in rotavirus-specific IgA and IgM PCs isolated from the GI mucosa (31). Lastly, rearrangements involving V5-51 were common in IgA PCs recognizing tissue transglutaminase in the GI mucosa of patients with celiac disease (32). When these IgHV genes were examined here, TLR activation was found to decrease the relative frequencies of B cells using V1-69 and V5-51, while CD40L/IL-21 did not show such an association (mutated repertoire Figure 4B, non-mutated and total repertoires Supplemental Figure 1). Other IgHV genes were altered as per Supplementary Table II.

The IgH locus shows convergent BCR composition following TLR stimulation

As the CDR3 is the most variable portion of the IgH and is essential for antigen recognition (33), we then determined the influence of TLR and CD40/IL-21 signals on promoting

sharing of CDR3 sequences. For this we examined equally sized subsets of the overall repertoire for each donor for each condition. Following either TLR9 or TLR/IFN stimulation, B cell cultures of individual donors shared up to 4% of their sequences (Figure 5). In contrast, CD40L/IL-21 B cell activation did not induce CDR3 sharing, instead promoting proliferation of separate B cell populations. Patterns of sequence sharing were recapitulated when relative sequence frequencies were factored in (not shown). These findings suggest that TLR stimuli activate similar B cells, leading to survival or expansion of cells that might be expected to produce antibodies with similar antigen specificities. While individuals shared specific rearrangements, we point out that sharing of identical sequences between donors was minimal, likely due to the vast sequence diversity at baseline.

Somatically hypermutated sequences expand following TLR stimulation

The sequence similarity induced by TLR stimulation suggests that some B cells might respond to TLR activation more strongly than others, unlike B cells activated by CD40L/IL-21. To characterize these differences, we first examined patterns of somatic hypermutation (SHM), defined as two or more mutations in the IgHV nucleotide sequence. TLR stimulation increased the proportion of mutated sequences while CD40L/IL-21 stimulation did not (Figure 6), with similar findings obtained when considering relative sequence frequency. Among mutated sequences, however, the extent of mutation was not significantly affected by any stimulation, both when assessed per donor or per IgHV family (not shown). As such, TLR stimulation likely expanded B cells that were mutated at baseline.

TLR stimulation expands B cells bearing shorter and less negatively charged CDR3 segments

Due to its importance for antigen recognition, the construction of the CDR3 was assessed. We noted that the mean CDR3 length decreased for TLR9 and TLR/IFN stimulated B cells, while CD40L/IL-21 stimulation failed to induce length changes. These TLR induced changes were entirely contained within the mutated sequence subset where, on average, half of a codon was lost from the mean length of 15.3 residues (Figure 7A). When relative sequence frequencies were considered, the CDR3 segments of mutated sequences from TLR9 and TLR/IFN stimulated cells were shortened by two thirds of a codon from a mean of 15.3 residues. To better understand these differences, frequency distributions of CDR3 lengths of mutated sequences were examined, revealing an expansion of shorter CDR3 segments following TLR stimulation that was not seen following treatment with CD40L/IL-21 (Figure 7B). Similar changes were not consistently found among the nonmutated sequence repertoires (Supplementary Figure 2).

TLR9 and TLR/IFN stimulation also expanded B cells bearing less negatively charged CDR3 segments (Figures 8A non-mutated, 8B mutated subset). The TLR-induced changes would be likely to impact antigen recognition as they represented large percent increases relative to the mean charge of unstimulated cells, with increases of 37 to 63 percent for unique sequences and increases of 45 to 80 percent when considering relative sequence frequencies. In contrast, CD40L/IL-21 stimulation weakly promoted increasingly negative

charges in nonmutated B cells, trending towards an average reduction of 23% relative to the mean charge of unstimulated cells. To better understand these changes, the proportions of sequences bearing specific CDR3 charges were determined, revealing TLR-driven expansion of B cells bearing CDR3s with net charges of 1 to 3 in non-mutated sequences, compared to CDR3s of net charge of 1 in mutated sequences (not shown). As expected by the changes in charge, TLR stimulation decreased CDR3 acidic residues and increased CDR3 basic residues, with all amino acids in each group contributing to the differences (not shown).

TLR stimulation induces CDR3 profiles consistent with anti-nuclear reactivity as well as autoreactive antibodies

For all cultures, longer CDR3 segments were more negatively charged than shorter CDR3s. As TLR stimulation both shortened the CDR3 and increased the charge towards positive, we next assessed CDR3 charge among segments of equal length, finding that the magnitude of TLR-induced increase in charge was positively correlated with CDR3 length (Figure 9A).

Longer and positively charged CDR3 segments have previously been associated with autoreactivity (34). As TLR stimulation favored the emergence of such CDR3s, we tested whether the antibodies secreted following stimulation bound to HEp-2 cells. Culture supernatants from TLR9 and TLR/IFN stimulated cultures showed robust reactivity, unlike cultures activated by CD40L/IL-21 (representative images 9B, summary 9C). Given the expansion noted in IgM+ populations by flow cytometry, HEp-2 binding by IgM isotype antibodies was specifically assessed, showing robust binding by antibodies secreted following TLR9 and TLR/IFN stimulation (Figure 9D). For both sets of slides, the strongest staining was cytoplasmic, consistent with tropomyosin or cytokeratin patterns, which overlaid a weaker nuclear staining consistent with centromere associated proteins, nuclear matrix, MSA-2 midbody, or nuclear rim patterns.

Discussion

This study examined peripheral blood B cell responses of four donors to stimulation through TLR7 and TLR9, defining TLR responsive B cells based on phenotype, immunoglobulin secretion, and BCR structure. In contrast to CD40L/IL-21 stimulation, TLRs expanded IgM positive B cells from $CD27^{+}$ memory and $CD27^{hi}$ PC lineage committed populations (15). TLR activation drove responding cells primarily towards secretion of IgM, unlike CD40L/IL-21 stimulation that induced relatively more balanced IgM and IgG production. Perhaps contributing to this difference, CD40L/IL-21 induced proliferation of virtually all memory and most naïve B cells, while TLRs induced proliferation of a subset of these cells. TLR responsive B cells shared BCR structure, showing characteristic patterns of IgHV and IgHJ usage, particularly in mutated sequences. Given their history of somatic hypermutation (SHM), these sequences likely originated from memory B cells, as shown in older studies of sorted cells (35). Stimulation through TLRs, but not CD40L/IL-21, also expanded shared CDR3 sequences, indicating that a common subset of B cells may have responded to these stimuli. TLR responding cells were more likely to have mutated BCRs, and had shorter CDR3 segments bearing less negative charge. Interestingly, the magnitude of the TLR-

induced increase in charge correlated with CDR3 length, resulting in a more positive charge amongst longer CDR3 segments. Of note, these TLR effects were found for each donor, showing similar patterns and magnitudes of effect, suggesting that TLR stimulation may commonly drive the survival and proliferation of a subset of human B cells. In contrast, B cells stimulated with CD40L/IL-21, which also induced proliferation, differentiation, and Ig secretion, genetically resembled the unstimulated samples, indicating that TLR induced changes are unique and are not general consequences of B cell activation.

While stimulation through TLR7, especially at the low doses used, is a weak activator of B cells, we noted that TLR7 and TLR9 or TLR/IFN stimulation resulted in similar promotion of IgM+ responses. As noted previously, responses to TLR7 stimulation were robust when the receptor levels were boosted by IFNα (1), leading to responses resembling those noted for TLR9 stimulation.

Both TLR and CD40L/IL-21 stimulation are able to drive commitment into PC lineage and Ig secretion, yet TLR stimulation biased both processes towards the IgM isotype relative to activation by CD40L/IL-21. A high dose TLR9 agonist, in conjunction with BCR ligation, was previously reported to favor IgM secretion (36), results which are expanded here to include IgM induction following low dose stimulation solely through TLR9 or TLR7. This TLR skewing of responses towards IgM raises the possibility that TLR responsive B cells could have special effector responses, such as complement fixation or mucosal protection, for which IgM is quite suitable

We found that IgM memory B cells, a heterogeneous mix of circulating splenic marginal zone B cells (37) and B cells originating from both GC-dependent and GC-independent activation (38), were particularly responsive to TLR activation. In support, more than half of TLR-induced changes in IgHV gene usage match previously published gene usage patterns found to differentiate IgM memory cells from naïve or class-switched memory populations (39). IgM+ memory B cells are potentially dependent on MyD88 signaling as patients with inborn errors in MyD88 and IRAK4 have reduced numbers of these cells (7, 40). The roles of endosomal TLR7 and TLR9 in promoting this subset are less clear, however, as two patients deficient in the TLR endosomal trafficker UNC93B1 had normal numbers of IgM+ memory B cells, although these cells showed lower levels of SHM (40). As TLR9 activation induced mutated IgM memory cells from cord-blood derived transitional B cells (41) and as we found TLRs to expand both IgM memory cells and mutated sequences, our data suggest that a mutated subset of IgM memory cells could be particularly responsive to endosomal TLRs, potentially explaining this reduction of IgM memory SHM in these few patients with UNC93B1 mutations.

While TLRs clearly expand B cells bearing mutated BCRs, our results suggest expansion of B cells mutated at baseline over *in vitro* induction of mutations. Aranburu et. al. previously reported a TLR9-dependent induction of mutations in IgHV1 and IgHV4/6, but not IgHV5, in cord-blood derived transitional B cells (41). In contrast, we found no IgHV-specific differences in extent of mutation in total B cell populations following TLR stimulation. As the previous study assessed cells at an earlier stage of differentiation, used a higher concentration of TLR9 agonist in concert with BCR ligation, focused on proliferating cells,

and sequenced single cells, the differences in results are perhaps not surprising. While factoring in proliferation did not alter our results, it remains possible that *de novo* mutations were specifically introduced in dividing B cells. More likely, however, is that this difference reflects response patterns of adult peripheral blood B cells as opposed to cord blood B cells.

For each donor, TLR stimulation promoted positive charges among longer CDR3 segments, reminiscent of autoreactive antibodies (34). Accordingly, we found that TLR activation promoted autoantibody secretion from B cells of these healthy individuals, findings previously described for autoimmune prone mice (42–45) and humans with autoimmunity (46–48). While roughly one quarter of healthy individuals have autoreactive antibodies detectable in serum (49), in these experiments TLR stimulation induced detectable autoantibodies in culture supernatants of all donors, including IgM isotype autoantibodies. These data were somewhat unexpected based on earlier reports which found IgG+ memory B cells to have high rates of autoreactivity while IgM+ memory populations had virtually none (50). There are, however, significant methodological differences between our study, where we assess the antibodies secreted in response to stimulation, and earlier studies that examined the reactivity of antibodies cloned from single B cells. As such, the difference in results is perhaps not surprising. Follow up studies to assess the profile of antibodies secreted by various B cell populations in response to TLR stimulation will be required to fully examine these differences.

As has been pointed out elsewhere, autoreactivity can also be protective, as is the case for many natural antibodies (NA) which may ameliorate autoimmunity (51, 52) and help maintain homeostasis (51). IgM NA are often positively charged to facilitate interaction with negatively charged targets (53), and may have high levels of poly-reactivity (54). Murine B1 cells secreting NA are also TLR-responsive (11, 55) and have unique BCR construction (56), making them distinct from pathogenic antinuclear autoantibody producing cells (57). As a human analogue of B1 cells has not been definitively described (58–63), human NA-secreting B cells are not as well understood, though IgM memory B cells have been proposed as a source of these antibodies (37, 64). Potentially, the TLR responsive cells identified here are cells of this lineage in spite of the reduced frequencies of V1-69 noted following TLR stimulation.

The selectivity of TLR responsiveness among B cells has implications for the emerging field of TLR9 based vaccine adjuvants, as reviewed in (65, 66). Developing such agonists has been actively pursued, both in mice (67) and in small phase I/II studies in humans (68, 69). In humans, TLR9 adjuvants both boosted and modulated the immune response, increasing IgG1 and IgG3 but reducing IgG4 responses in one report, and transiently elevating anti-DNA antibodies in a few subjects in both reports (68, 69). Based on results presented here, TLR-based adjuvants might also drive secretion of antibodies of additional, and potentially autoreactive, specificities; however the extent to which TLR responsive B cells could be directly activated *in vivo* by TLR adjuvants remains unclear. Closer study of TLR-responsive B cells and of antibodies induced by TLR stimulation, both *in vitro* and *in vivo*, are needed to better understand the impact of such stimulation on human B cells.

Supplementary Material

Refer to Web version on PubMed Central for supplementary material.

Acknowledgments

Grant Support:

This work was supported by grants from the National Institutes of Health, AI 1061093, AI-349 0860037, AI-1048693, T32-GM007280, The Jeffrey Modell Foundation, and the David S Gottesman Immunology Chair.

This work was supported in part through the computational resources and staff expertise provided by the Department of Scientific Computing at the Icahn School of Medicine at Mount Sinai. Microscopy was performed at the Microscopy Shared Resource Facility at the Icahn School of Medicine at Mount Sinai.

Format for references

1. Bekeredjian-Ding IB, Wagner M, Hornung V, Giese T, Schnurr M, Endres S, Hartmann G. Plasmacytoid dendritic cells control TLR7 sensitivity of naive B cells via type I IFN. J Immunol. 2005; 174:4043–4050. [PubMed: 15778362]
2. Glaum MC, Narula S, Song D, Zheng Y, Anderson AL, Pletcher CH, Levinson AI. Toll-like receptor 7-induced naive human B-cell differentiation and immunoglobulin production. J Allergy Clin Immunol. 2009; 123:224–230.e224. [PubMed: 18995892]
3. He B, Qiao X, Cerutti A. CpG DNA induces IgG class switch DNA recombination by activating human B cells through an innate pathway that requires TLR9 and cooperates with IL-10. J Immunol. 2004; 173:4479–4491. [PubMed: 15383579]
4. Bernasconi NL, Onai N, Lanzavecchia A. A role for Toll-like receptors in acquired immunity: up-regulation of TLR9 by BCR triggering in naive B cells and constitutive expression in memory B cells. Blood. 2003; 101:4500–4504. [PubMed: 12560217]
5. Giordani L, Sanchez M, Libri I, Quaranta MG, Mattioli B, Viora M. IFN-alpha amplifies human naive B cell TLR-9-mediated activation and Ig production. J Leukoc Biol. 2009; 86:261–271. [PubMed: 19401392]
6. Capolunghi F, Cascioli S, Giorda E, Rosado MM, Plebani A, Auriti C, Seganti G, Zuntini R, Ferrari S, Cagliuso M, Quinti I, Carsetti R. CpG drives human transitional B cells to terminal differentiation and production of natural antibodies. J Immunol. 2008; 180:800–808. [PubMed: 18178818]
7. Maglione PJ, Simchoni N, Black S, Radigan L, Overbey JR, Bagiella E, Bussel JB, Bossuyt X, Casanova JL, Meyts I, Cerutti A, Picard C, Cunningham-Rundles C. IRAK-4- and MyD88-deficiencies impair IgM responses against T-independent bacterial antigens. Blood. 2014
8. So NS, Ostrowski MA, Gray-Owen SD. Vigorous response of human innate functioning IgM memory B cells upon infection by Neisseria gonorrhoeae. J Immunol. 2012; 188:4008–4022. [PubMed: 22427638]
9. Gunn KE, Brewer JW. Evidence that marginal zone B cells possess an enhanced secretory apparatus and exhibit superior secretory activity. J Immunol. 2006; 177:3791–3798. [PubMed: 16951340]
10. Martin F, Oliver AM, Kearney JF. Marginal zone and B1 B cells unite in the early response against T-independent blood-borne particulate antigens. Immunity. 2001; 14:617–629. [PubMed: 11371363]
11. Genestier L, Taillardet M, Mondiere P, Gheit H, Bella C, Defrance T. TLR agonists selectively promote terminal plasma cell differentiation of B cell subsets specialized in thymus-independent responses. J Immunol. 2007; 178:7779–7786. [PubMed: 17548615]
12. Fagarasan S, Watanabe N, Honjo T. Generation, expansion, migration and activation of mouse B1 cells. Immunol Rev. 2000; 176:205–215. [PubMed: 11043779]
13. Gray D, MacLennan IC, Bazin H, Khan M. Migrant mu+ delta+ and static mu+ delta- B lymphocyte subsets. Eur J Immunol. 1982; 12:564–569. [PubMed: 6811288]

14. Oliver AM, Martin F, Kearney JF. IgMhighCD21high lymphocytes enriched in the splenic marginal zone generate effector cells more rapidly than the bulk of follicular B cells. J Immunol. 1999; 162:7198–7207. [PubMed: 10358166]
15. Avery DT, Ellyard JI, Mackay F, Corcoran LM, Hodgkin PD, Tangye SG. Increased expression of CD27 on activated human memory B cells correlates with their commitment to the plasma cell lineage. J Immunol. 2005; 174:4034–4042. [PubMed: 15778361]
16. Zotos D, Coquet JM, Zhang Y, Light A, D'Costa K, Kallies A, Corcoran LM, Godfrey DI, Toellner KM, Smyth MJ, Nutt SL, Tarlinton DM. IL-21 regulates germinal center B cell differentiation and proliferation through a B cell-intrinsic mechanism. J Exp Med. 2010; 207:365–378. [PubMed: 20142430]
17. Alamyar E, Duroux P, Lefranc MP, Giudicelli V. IMGT(®) tools for the nucleotide analysis of immunoglobulin (IG) and T cell receptor (TR) V-(D)-J repertoires, polymorphisms, and IG mutations: IMGT/V-QUEST and IMGT/HighV-QUEST for NGS. Methods Mol Biol. 2012; 882:569–604. [PubMed: 22665256]
18. Munshaw S, Kepler TB. SoDA2: a Hidden Markov Model approach for identification of immunoglobulin rearrangements. Bioinformatics. 2010; 26:867–872. [PubMed: 20147303]
19. Team, RC. R: A Language and Environment for Statistical Computing. R Foundation for Statistical Computing; Vienna, Austria: 2014.
20. RStudio. RStudio: Integrated development environment for R. 2012.
21. Wickham H. The Split-Apply-Combine Strategy for Data Analysis. Journal of Statistical Software. 2011:40.
22. Wickham, H. ggplot2: elegant graphics for data analysis. Springer; New York: 2009.
23. Wickham H. Reshaping data with the reshape package. Journal of Statistical Software. 2007:21.
24. Maechler, M.; Rousseeuw, P.; Struyf, A.; Hubert, M.; Hornik, K. cluster: Cluster Analysis Basics and Extensions. 2014.
25. Carlson CS, Emerson RO, Sherwood AM, Desmarais C, Chung MW, Parsons JM, Steen MS, LaMadrid-Herrmannsfeldt MA, Williamson DW, Livingston RJ, Wu D, Wood BL, Rieder MJ, Robins H. Using synthetic templates to design an unbiased multiplex PCR assay. Nat Commun. 2013; 4:2680. [PubMed: 24157944]
26. Throsby M, van den Brink E, Jongeneelen M, Poon LL, Alard P, Cornelissen L, Bakker A, Cox F, van Deventer E, Guan Y, Cinatl J, ter Meulen J, Lasters I, Carsetti R, Peiris M, de Kruif J, Goudsmit J. Heterosubtypic neutralizing monoclonal antibodies cross-protective against H5N1 and H1N1 recovered from human IgM+ memory B cells. PLoS One. 2008; 3:e3942. [PubMed: 19079604]
27. Johnson TA, Rassenti LZ, Kipps TJ. Ig VH1 genes expressed in B cell chronic lymphocytic leukemia exhibit distinctive molecular features. J Immunol. 1997; 158:235–246. [PubMed: 8977195]
28. Seifert M, Steimle-Grauer SA, Goossens T, Hansmann ML, Bräuninger A, Küppers R. A model for the development of human IgD-only B cells: Genotypic analyses suggest their generation in superantigen driven immune responses. Mol Immunol. 2009; 46:630–639. [PubMed: 18952293]
29. Dal-Bo M, Del Giudice I, Bomben R, Capello D, Bertoni F, Forconi F, Laurenti L, Rossi D, Zucchetto A, Pozzato G, Marasca R, Efremov DG, Guarini A, Del Poeta G, Foà R, Gaidano G, Gattei V. B-cell receptor, clinical course and prognosis in chronic lymphocytic leukaemia: the growing saga of the IGHV3 subgroup gene usage. Br J Haematol. 2011; 153:3–14. [PubMed: 21303354]
30. Thorpe SJ, Turner CE, Stevenson FK, Spellerberg MB, Thorpe R, Natvig JB, Thompson KM. Human monoclonal antibodies encoded by the V4–34 gene segment show cold agglutinin activity and variable multireactivity which correlates with the predicted charge of the heavy-chain variable region. Immunology. 1998; 93:129–136. [PubMed: 9536129]
31. Di Niro R, Mesin L, Raki M, Zheng NY, Lund-Johansen F, Lundin KE, Charpilienne A, Poncet D, Wilson PC, Sollid LM. Rapid generation of rotavirus-specific human monoclonal antibodies from small-intestinal mucosa. J Immunol. 2010; 185:5377–5383. [PubMed: 20935207]
32. Di Niro R, Mesin L, Zheng NY, Stamnaes J, Morrissey M, Lee JH, Huang M, Iversen R, du Pré MF, Qiao SW, Lundin KE, Wilson PC, Sollid LM. High abundance of plasma cells secreting

transglutaminase 2-specific IgA autoantibodies with limited somatic hypermutation in celiac disease intestinal lesions. Nat Med. 2012; 18:441–445. [PubMed: 22366952]

33. Xu JL, Davis MM. Diversity in the CDR3 region of V(H) is sufficient for most antibody specificities. Immunity. 2000; 13:37–45. [PubMed: 10933393]
34. Wardemann H, Yurasov S, Schaefer A, Young JW, Meffre E, Nussenzweig MC. Predominant autoantibody production by early human B cell precursors. Science. 2003; 301:1374–1377. [PubMed: 12920303]
35. Klein U, Rajewsky K, Kuppers R. Human immunoglobulin (Ig)M+IgD+ peripheral blood B cells expressing the CD27 cell surface antigen carry somatically mutated variable region genes: CD27 as a general marker for somatically mutated (memory) B cells. J Exp Med. 1998; 188:1679–1689. [PubMed: 9802980]
36. Poeck H, Wagner M, Battiany J, Rothenfusser S, Wellisch D, Hornung V, Jahrsdorfer B, Giese T, Endres S, Hartmann G. Plasmacytoid dendritic cells, antigen, and CpG-C license human B cells for plasma cell differentiation and immunoglobulin production in the absence of T-cell help. Blood. 2004; 103:3058–3064. [PubMed: 15070685]
37. Weller S, Braun MC, Tan BK, Rosenwald A, Cordier C, Conley ME, Plebani A, Kumararatne DS, Bonnet D, Tournilhac O, Tchernia G, Steiniger B, Staudt LM, Casanova JL, Reynaud CA, Weill JC. Human blood IgM “memory” B cells are circulating splenic marginal zone B cells harboring a prediversified immunoglobulin repertoire. Blood. 2004; 104:3647–3654. [PubMed: 15191950]
38. Berkowska MA, Driessen GJ, Bikos V, Grosserichter-Wagener C, Stamatopoulos K, Cerutti A, He B, Biermann K, Lange JF, van der Burg M, van Dongen JJ, van Zelm MC. Human memory B cells originate from three distinct germinal center-dependent and -independent maturation pathways. Blood. 2011; 118:2150–2158. [PubMed: 21690558]
39. Wu YC, Kipling D, Leong HS, Martin V, Ademokun AA, Dunn-Walters DK. High-throughput immunoglobulin repertoire analysis distinguishes between human IgM memory and switched memory B-cell populations. Blood. 2010; 116:1070–1078. [PubMed: 20457872]
40. Weller S, Bonnet M, Delagreverie H, Israel L, Chrabieh M, Maródi L, Rodriguez-Gallego C, Garty BZ, Roifman C, Issekutz AC, Zitnik SE, Hoarau C, Camcioglu Y, Vasconcelos J, Rodrigo C, Arkwright PD, Cerutti A, Meffre E, Zhang SY, Alcais A, Puel A, Casanova JL, Picard C, Weill JC, Reynaud CA. IgM+IgD+CD27+ B cells are markedly reduced in IRAK-4-, MyD88-, and TIRAP- but not UNC-93B-deficient patients. Blood. 2012; 120:4992–5001. [PubMed: 23002119]
41. Aranburu A, Ceccarelli S, Giorda E, Lasorella R, Ballatore G, Carsetti R. TLR ligation triggers somatic hypermutation in transitional B cells inducing the generation of IgM memory B cells. J Immunol. 2010; 185:7293–7301. [PubMed: 21078901]
42. Ehlers M, Fukuyama H, McGaha TL, Aderem A, Ravetch JV. TLR9/MyD88 signaling is required for class switching to pathogenic IgG2a and 2b autoantibodies in SLE. J Exp Med. 2006; 203:553–561. [PubMed: 16492804]
43. Celhar T, Magalhães R, Fairhurst AM. TLR7 and TLR9 in SLE: when sensing self goes wrong. Immunol Res. 2012; 53:58–77. [PubMed: 22434514]
44. Christensen SR, Shupe J, Nickerson K, Kashgarian M, Flavell RA, Shlomchik MJ. Toll-like receptor 7 and TLR9 dictate autoantibody specificity and have opposing inflammatory and regulatory roles in a murine model of lupus. Immunity. 2006; 25:417–428. [PubMed: 16973389]
45. Nickerson KM, Christensen SR, Shupe J, Kashgarian M, Kim D, Elkon K, Shlomchik MJ. TLR9 regulates TLR7- and MyD88-dependent autoantibody production and disease in a murine model of lupus. J Immunol. 184:1840–1848. [PubMed: 20089701]
46. Chauhan SK, Singh VV, Rai R, Rai M, Rai G. Distinct autoantibody profiles in systemic lupus erythematosus patients are selectively associated with TLR7 and TLR9 upregulation. J Clin Immunol. 2013; 33:954–964. [PubMed: 23564191]
47. Laska MJ, Troldborg A, Hansen B, Stengaard-Pedersen K, Junker P, Nexø BA, Voss A. Polymorphisms within Toll-like receptors are associated with systemic lupus erythematosus in a cohort of Danish females. Rheumatology (Oxford). 2014; 53:48–55. [PubMed: 24064706]
48. Mu R, Sun XY, Lim LT, Xu CH, Dai CX, Su Y, Jia RL, Li ZG. Toll-like receptor 9 is correlated to disease activity in Chinese systemic lupus erythematosus population. Chin Med J (Engl). 2012; 125:2873–2877. [PubMed: 22932083]

49. Wandstrat AE, Carr-Johnson F, Branch V, Gray H, Fairhurst AM, Reimold A, Karp D, Wakeland EK, Olsen NJ. Autoantibody profiling to identify individuals at risk for systemic lupus erythematosus. J Autoimmun. 2006; 27:153–160. [PubMed: 17052888]
50. Tiller T, Tsuiji M, Yurasov S, Velinzon K, Nussenzweig MC, Wardemann H. Autoreactivity in human IgG+ memory B cells. Immunity. 2007; 26:205–213. [PubMed: 17306569]
51. Grönwall C, Vas J, Silverman GJ. Protective Roles of Natural IgM Antibodies. Front Immunol. 2012; 3:66. [PubMed: 22566947]
52. Mannoor K, Matejuk A, Xu Y, Beardall M, Chen C. Expression of natural autoantibodies in MRL-lpr mice protects from lupus nephritis and improves survival. J Immunol. 2012; 188:3628–3638. [PubMed: 22407922]
53. Chikazawa M, Otaki N, Shibata T, Miyashita H, Kawai Y, Maruyama S, Toyokuni S, Kitaura Y, Matsuda T, Uchida K. Multispecificity of immunoglobulin M antibodies raised against advanced glycation end products: involvement of electronegative potential of antigens. J Biol Chem. 2013; 288:13204–13214. [PubMed: 23543734]
54. Mannoor K, Xu Y, Chen C. Natural Autoantibodies and Associated B Cells in Immunity and Autoimmunity. Autoimmunity. 2012
55. Gururajan M, Jacob J, Pulendran B. Toll-like receptor expression and responsiveness of distinct murine splenic and mucosal B-cell subsets. PLoS One. 2007; 2:e863. [PubMed: 17848994]
56. Tornberg UC, Holmberg D. B-1a, B-1b and B-2 B cells display unique VHDJH repertoires formed at different stages of ontogeny and under different selection pressures. EMBO J. 1995; 14:1680–1689. [PubMed: 7737121]
57. Reap EA, Sobel ES, Cohen PL, Eisenberg RA. Conventional B cells, not B-1 cells, are responsible for producing autoantibodies in lpr mice. J Exp Med. 1993; 177:69–78. [PubMed: 8418209]
58. Descatoire M, Weill JC, Reynaud CA, Weller S. A human equivalent of mouse B-1 cells? J Exp Med. 2011; 208:2563–2564. author reply 2566–2569. [PubMed: 22184680]
59. Perez-Andres M, Grosserichter-Wagener C, Teodosio C, van Dongen JJ, Orfao A, van Zelm MC. The nature of circulating CD27+CD43+ B cells. J Exp Med. 2011; 208:2565–2566. author reply 2566–2569. [PubMed: 22184681]
60. Griffin DO, Holodick NE, Rothstein TL. Human B1 cells in umbilical cord and adult peripheral blood express the novel phenotype CD20+ CD27+ CD43+ CD70- J Exp Med. 2011; 208:67–80. [PubMed: 21220451]
61. Reynaud CA, Weill JC. Gene profiling of $CD11b^{+}$ and $CD11b^{-}$ B1 cell subsets reveals potential cell sorting artifacts. J Exp Med. 2012; 209:433–434. author reply 434–436. [PubMed: 22412175]
62. Tangye SG. To B1 or not to B1: that really is still the question! Blood. 2013; 121:5109–5110. [PubMed: 23813936]
63. Covens K, Verbinnen B, Geukens N, Meyts I, Schuit F, Van Lommel L, Jacquemin M, Bossuyt X. Characterization of proposed human B-1 cells reveals pre-plasmablast phenotype. Blood. 2013; 121:5176–5183. [PubMed: 23613519]
64. Cerutti A, Cols M, Puga I. Marginal zone B cells: virtues of innate-like antibody-producing lymphocytes. Nat Rev Immunol. 2013; 13:118–132. [PubMed: 23348416]
65. Vollmer J, Krieg AM. Immunotherapeutic applications of CpG oligodeoxynucleotide TLR9 agonists. Adv Drug Deliv Rev. 2009; 61:195–204. [PubMed: 19211030]
66. Bode C, Zhao G, Steinhagen F, Kinjo T, Klinman DM. CpG DNA as a vaccine adjuvant. Expert Rev Vaccines. 2011; 10:499–511. [PubMed: 21506647]
67. Gungor B, Yagci FC, Tincer G, Bayyurt B, Alpdundar E, Yildiz S, Ozcan M, Gursel I, Gursel M. CpG ODN Nanorings Induce IFNα from Plasmacytoid Dendritic Cells and Demonstrate Potent Vaccine Adjuvant Activity. Sci Transl Med. 2014; 6:235ra261.
68. Cooper CL, Davis HL, Morris ML, Efler SM, Adhami MA, Krieg AM, Cameron DW, Heathcote J. CPG 7909, an immunostimulatory TLR9 agonist oligodeoxynucleotide, as adjuvant to Engerix-B HBV vaccine in healthy adults: a double-blind phase I/II study. J Clin Immunol. 2004; 24:693–701. [PubMed: 15622454]
69. Cooper CL, Davis HL, Angel JB, Morris ML, Elfer SM, Seguin I, Krieg AM, Cameron DW. CPG 7909 adjuvant improves hepatitis B virus vaccine seroprotection in antiretroviral-treated HIV-infected adults. AIDS. 2005; 19:1473–1479. [PubMed: 16135900]

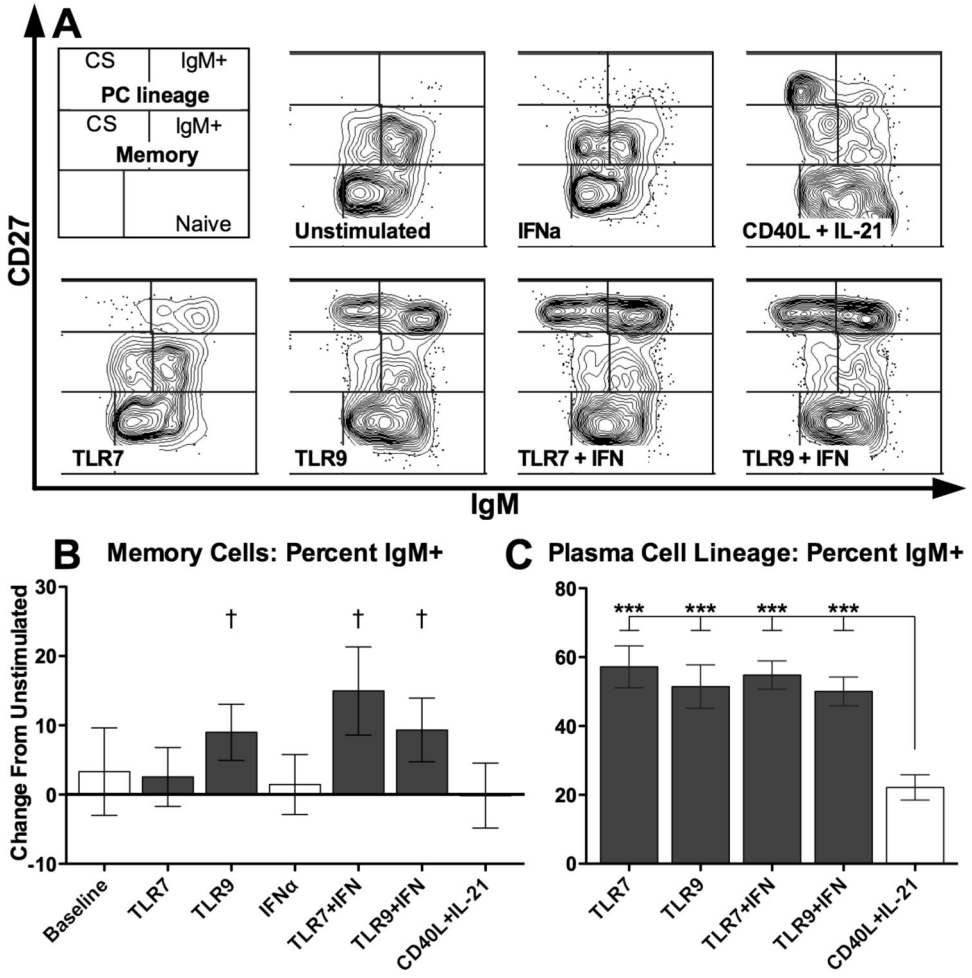

Figure 1. TLR stimulation of human B cells expands IgM+ memory cells and plasma cell lineage committed cells

A: Representative day 7 cultured cells characterized by flow cytometry, gated on live singlet cells. B: Within the $CD27^{+}$ memory gate, TLR stimulation expanded the proportion of IgM+ cells relative to the mean of 49% for unstimulated cells. C: Within the plasma cell lineage committed $CD27^{hi}$ gate, TLR stimulation expanded IgM+ cells, unlike CD40L/IL-21. B–C: bars represent mean, error bars represent SEM. † = $p < 0.1$; *** = $p < 0.001$; CS = class-switched, defined as IgM-; PC = plasma cell. A: representative figures from one donor out of four, with experiments performed in duplicate; B–C: summary of four independent donors with two replicates each.

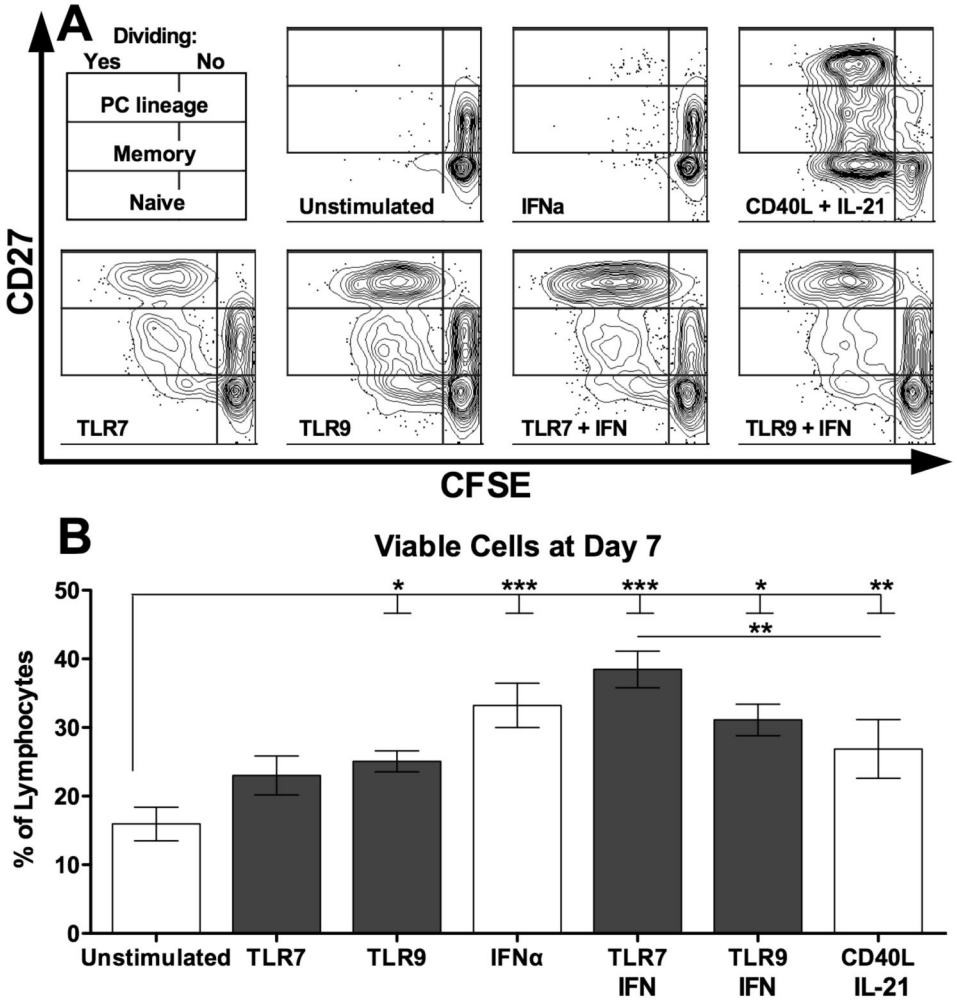

Figure 2. CD40L/IL-21 promotes proliferation of most B cells while TLR stimulation is selective

A: Representative day 7 cultured cells characterized by flow cytometry, gated on live singlet cells. B: The proportion of live cells did not differ among stimuli at day 7. B: bars represent mean, error bars represent SEM. * = $p < 0.05$; ** = $p < 0.01$; *** = $p < 0.001$; PC = plasma cell. A: representative figures from one donor out of two, with experiments performed in duplicate; B: summary of four independent donors with two replicates each.

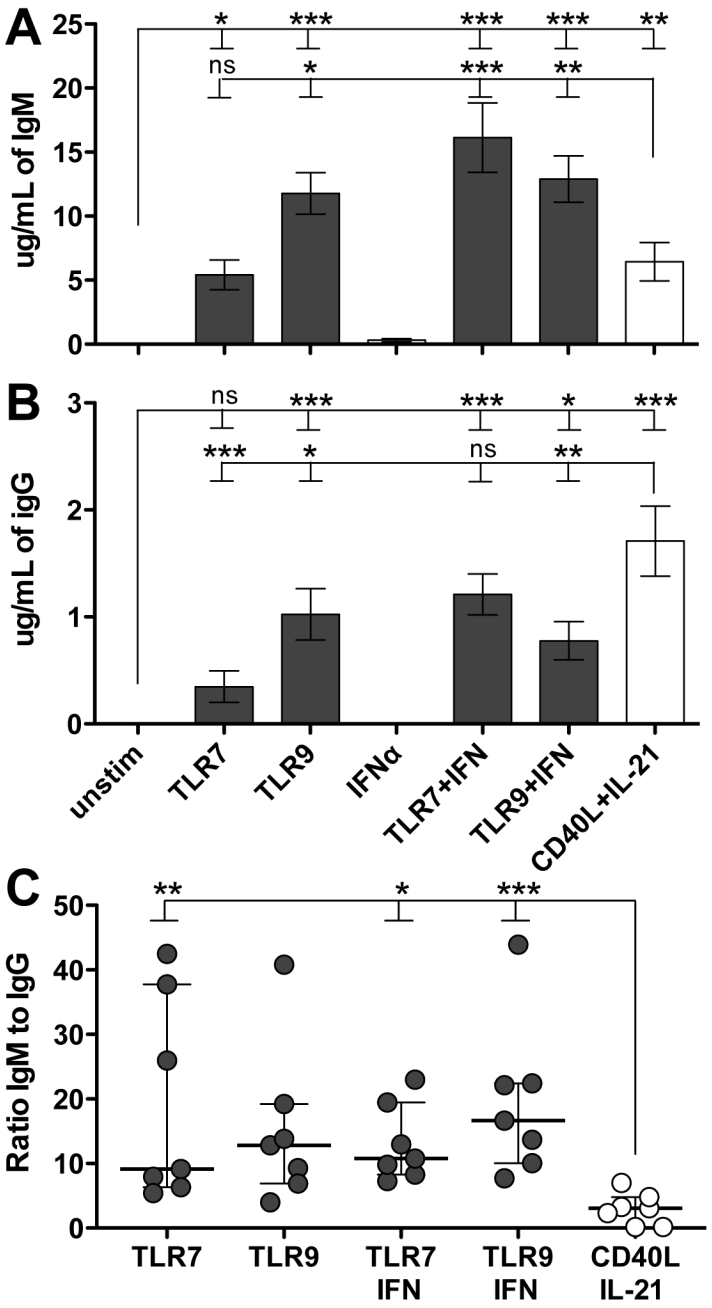

Figure 3. TLRs skews antibody secretion towards IgM

A: TLR9 and TLR/IFN stimulated cells secreted high levels of IgM. B: Stimulated B cells also secreted IgG, with CD40L/IL-21 inducing more robust secretion. C: TLR stimulation skewed responding B cells towards secreting higher levels of IgM relative to IgG. A–B: bars represent mean, error bars represent SEM. C: bar represents median, error bars represent IQR. ns = $p > 0.1$; * = $p < 0.05$; ** = $p < 0.01$; *** = $p < 0.001$; A–C: summary of four independent donors with two replicates each.

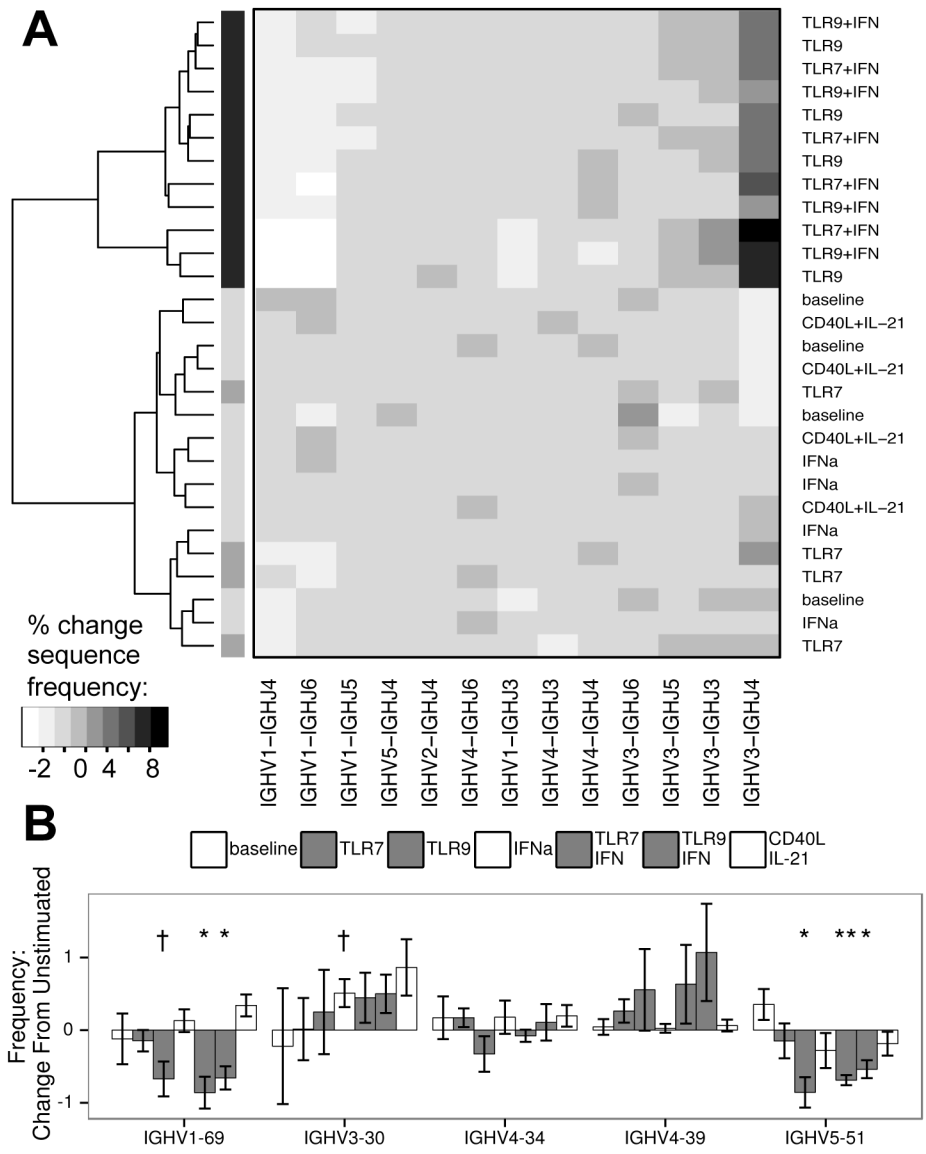

Figure 4. Deep Sequencing of the IgH locus reveals clustering of TLR stimulated cells based on V and J usage

A: Unbiased clustering of IgHV and IgHJ pairing frequencies of the mutated sequence subset, showing grouping of TLR9 and TLR/IFN (in black) stimulated samples from four donors in contrast to other cultures (dendrogram shading added for ease of viewing). To control for inter-donor differences and nonspecific changes due to culture, data were normalized based on unstimulated samples prior to clustering. B: Changes in frequency of IgHV genes of specific interest (see results section for description). A: Algorithm: complete clustering based on Euclidean distances for IgHV-IgHJ pairings, filtered on pairings with at least 1% change in frequency between any two samples. B: bars represent mean, error bars represent SEM. Columns appear in order of legend. † = $p < 0.1$; * = $p < 0.05$; ** = $p < 0.01$; A–B: data represent four independent donors, split across two independent sequencing runs.

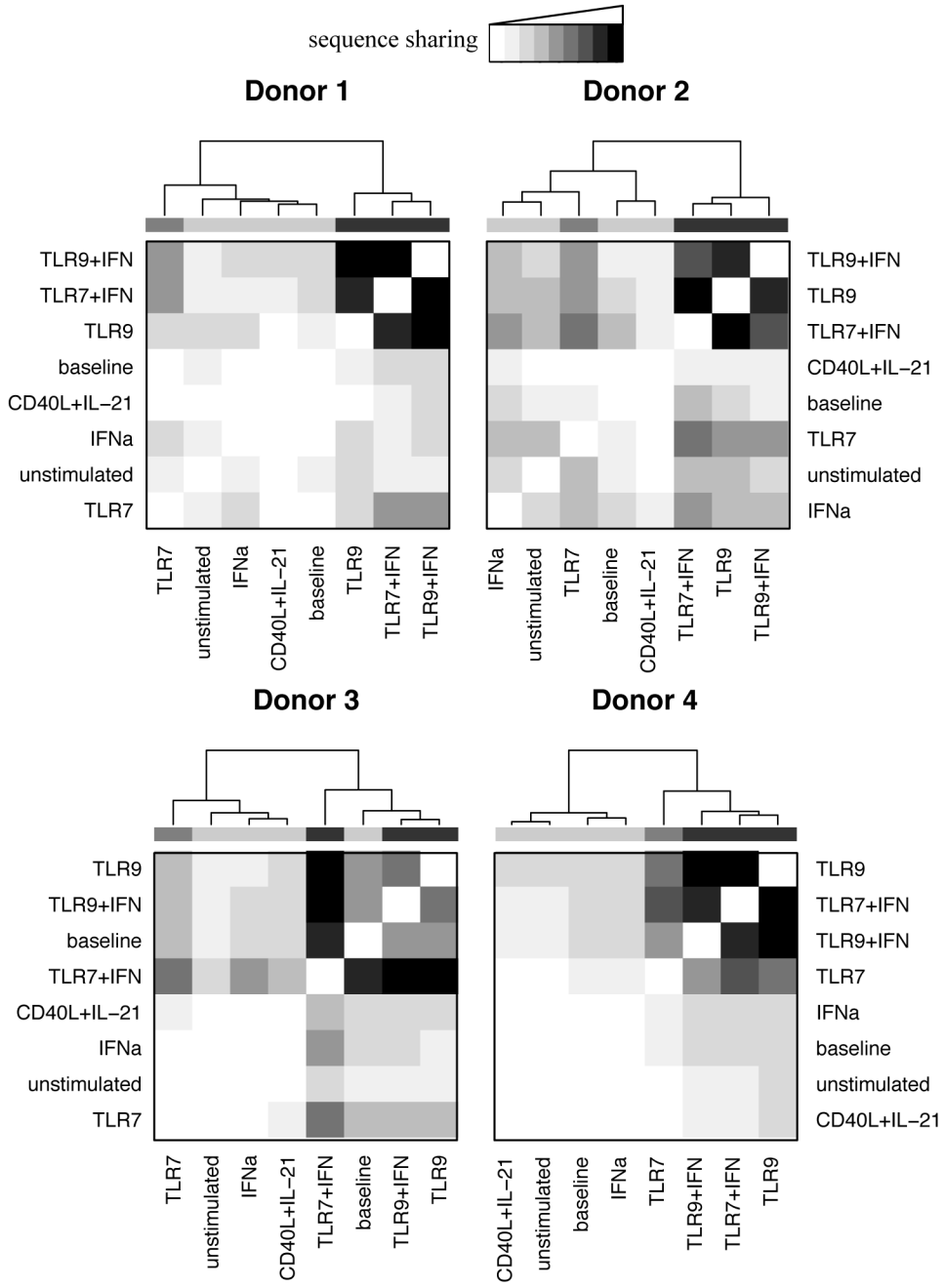

Figure 5. Deep sequencing of the IgH locus shows convergence of BCRs following TLR stimulation

TLR9 and TLR/IFN activated B cells of each donor demonstrated increased CDR3 amino acid sequence sharing following stimulation, while two similarly showed convergence following TLR7 stimulation (sequence sharing as indicated.) To control for differing sequencing depth, repertoire subsets of equal size were examined pair-wise for all samples from each donor, counting overlapping sequences. These counts were then clustered based on complete clustering of Euclidean distances, with dendrogram shading added for ease of viewing. The greatest extent of overlap represents 0.5%, 3.9%, 3.3%, and 1.75% sharing of

sequences for donors 1 through 4. Data represent four independent donors, split across two independent sequencing runs, with subsampling performed 5 times.

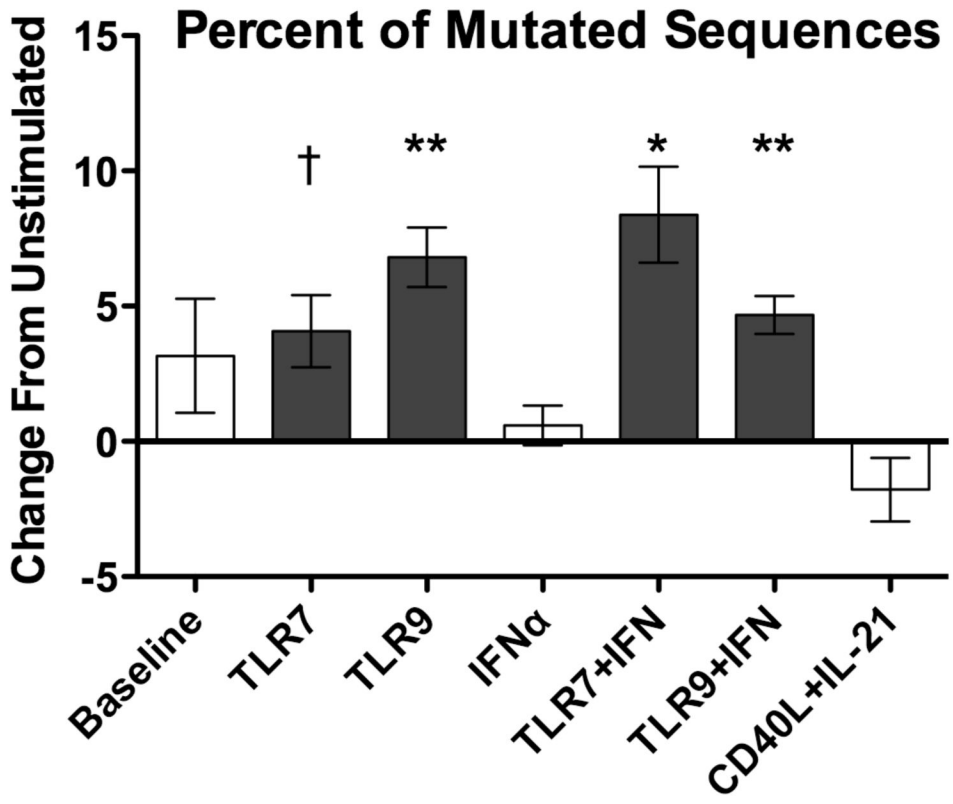

Figure 6. TLR stimulation expands mutated B cells

The proportion of somatically hypermutated sequences (2+ IgHV mutations) increased with TLR stimulation relative to mean proportion of 25% for unstimulated cells. CD40L/IL-21 stimulation did not change the proportion of mutated sequences. Plot indicates data normalized intra-donor to unstimulated cultures. Bars represent mean and error bars represent SEM. † = $p < 0.1$, * = $p < 0.05$, ** = $p < 0.01$. Data represent four independent donors, split across two independent sequencing runs.

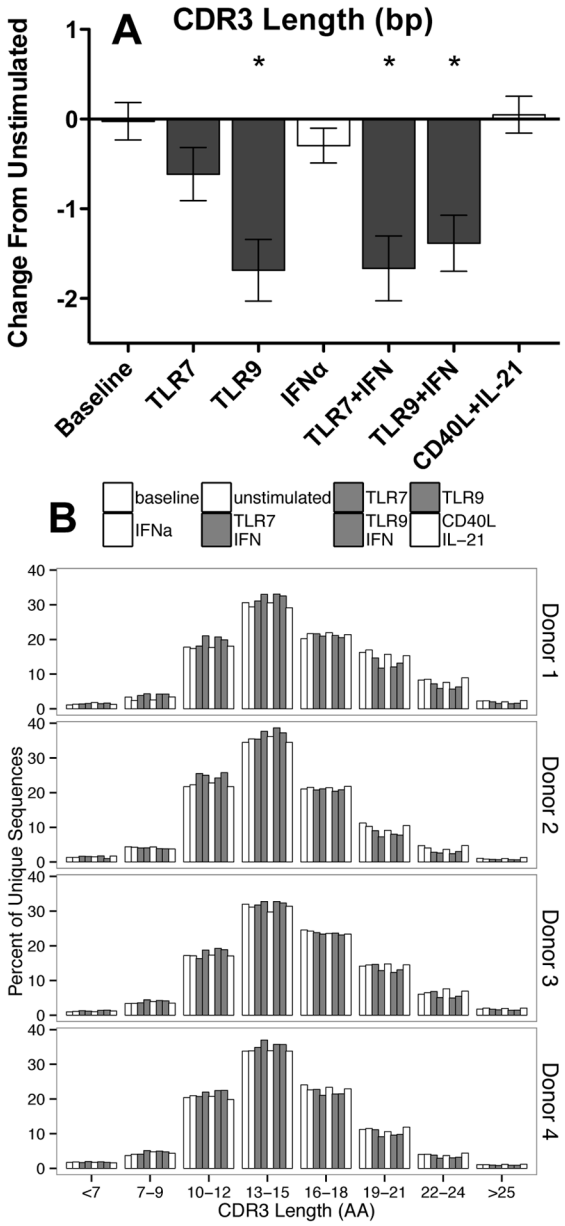

Figure 7. TLR stimulation expands cells bearing shorter CDR3 segments

A: TLR stimulation selectively expanded B cells with shorter CDR3 segments, particularly among mutated B cells, relative to mean length of 46 bases for unstimulated cells. B: TLR stimulation shifts the frequency distribution of CDR3 lengths towards shorter CDR3s. A: Bars represent mean, error bars represent SEM. B: bars represent sum of the proportion of unique sequences with a CDR3 length in the indicated length range. Columns appear in order of legend. * = $p < 0.05$. Data represent four independent donors, split across two independent sequencing runs.

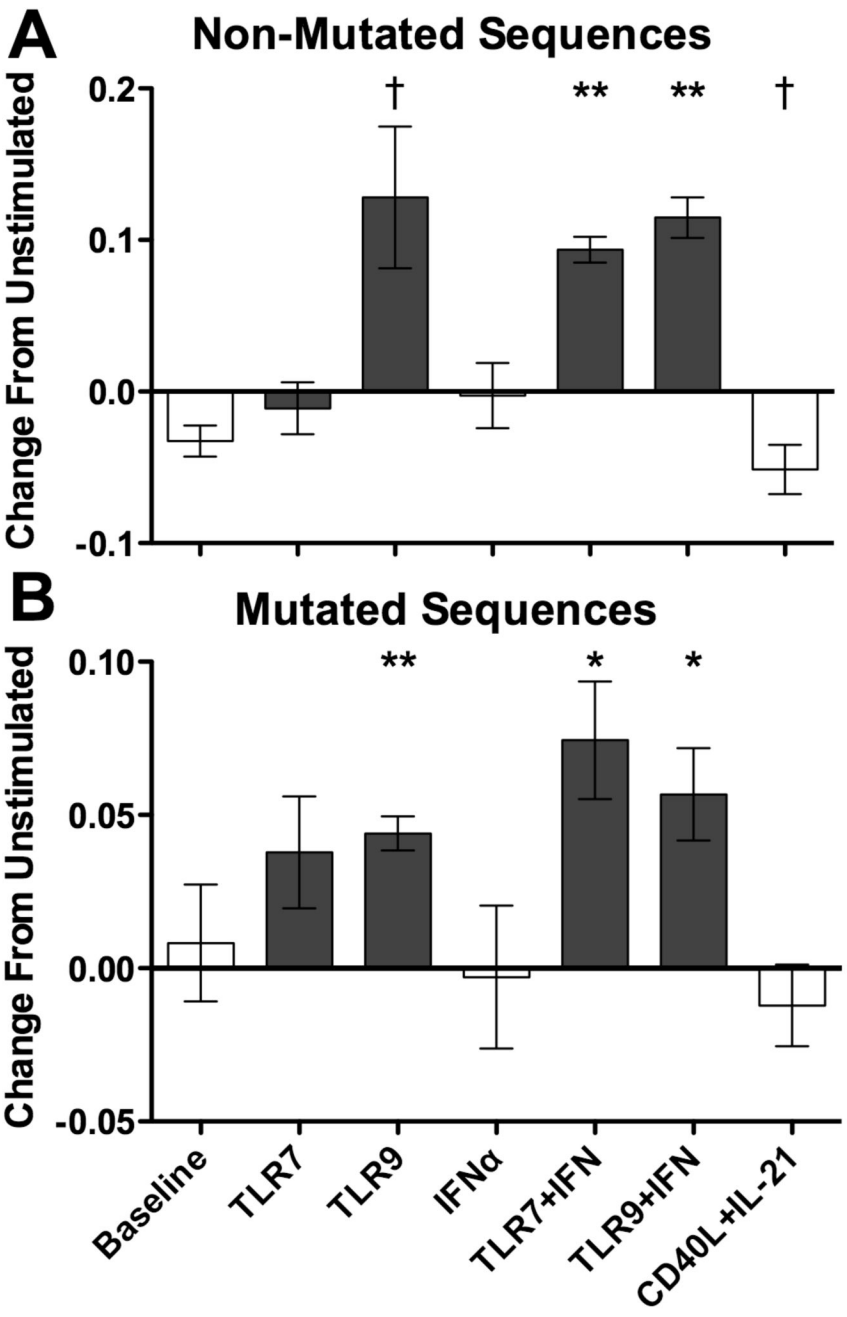

Figure 8. TLR stimulation expands cells bearing less negatively charged CDR3 segments

TLR9 and TLR/IFN stimulation induced less negatively charged CDR3 segments in both non-mutated (A) and mutated (B) sequence subsets relative to mean charges of -0.55 and -0.47 for unstimulated cells. Bars represent mean, error bars represent SEM. † = $p < 0.1$, * = $p < 0.05$, ** = $p < 0.01$. Data represent four independent donors, split across two independent sequencing runs.

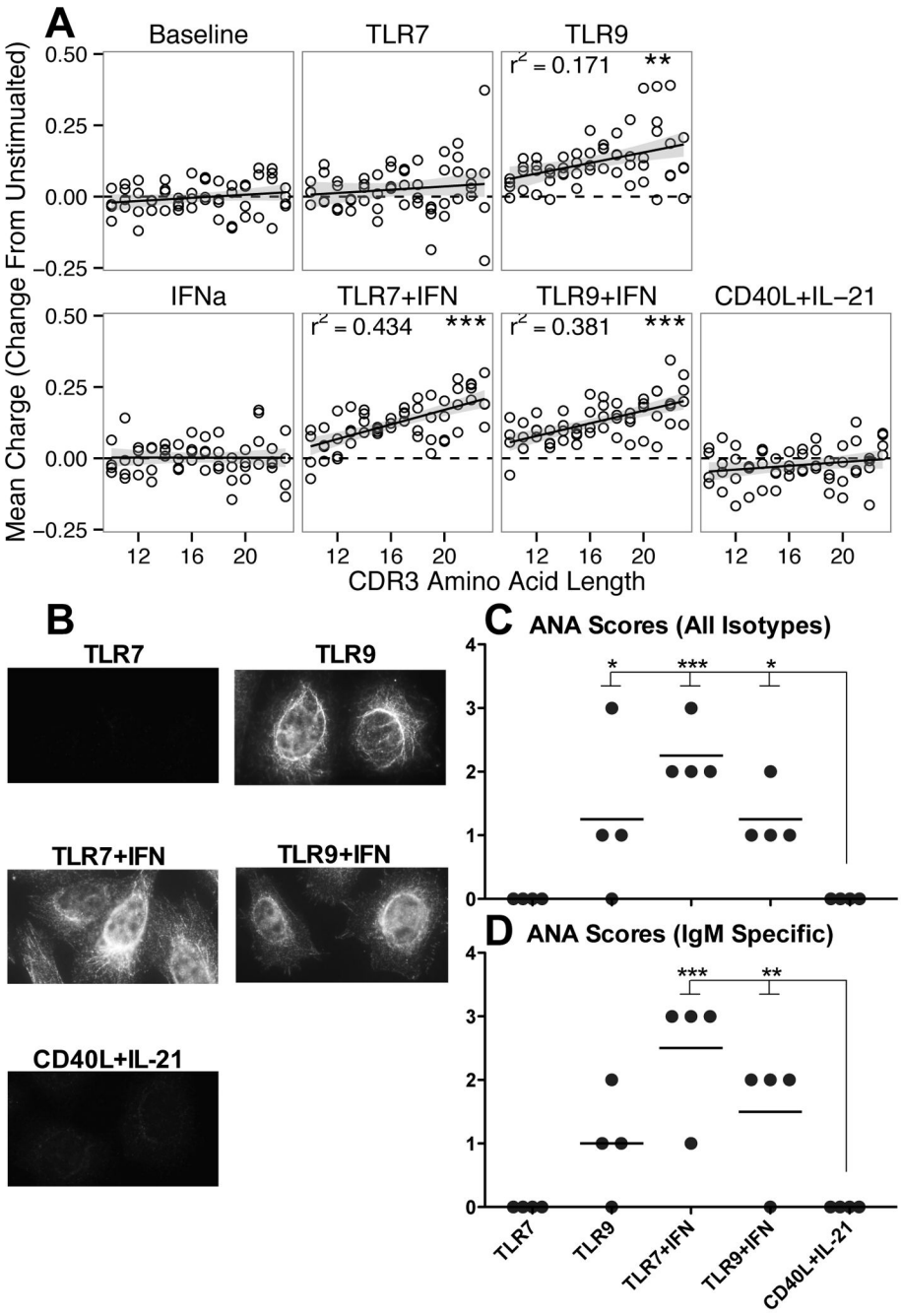

Figure 9. TLR stimulation induced autoreactive antibodies

A: TLR activation induced a mean charge increase that was positively correlated with CDR3 length. Plots indicate data normalized intra-donor to unstimulated cultures, and CDR3 length range represents modal 90% of lengths. Grey line represents 95% confidence interval tracing for linear model and dotted black line as reference for no change. r refers to Pearson correlation coefficient. B: Representative images obtained from probing culture supernatants for reactivity against HEp2 cells, showing induction of autoreactive antibodies following TLR stimulation. Summary of antinuclear staining scores for all donors using either anti-

light chain (C) or anti-IgM isotype (D) detection reagents. Supernatant reactivity was graded on a scale of 0 (negative) or 1+ (weak staining) through 4+ (intense staining). * = $p < 0.05$; ** = $p < 0.01$; *** = $p < 0.001$. A: Data represent four independent donors, split across two independent sequencing runs. B: representative images from one donor. C–D: summary of four independent donors, each with two slides stained.